

# NEURAL AUDIO FINGERPRINT FOR HIGH-SPECIFIC AUDIO RETRIEVAL BASED ON CONTRASTIVE LEARNING

Sungkyun Chang<sup>1</sup>, Donmoon Lee<sup>1,2</sup>, Jeongsoo Park<sup>1</sup>, Hyungui Lim<sup>1</sup>,  
Kyogu Lee<sup>2</sup>, Karam Ko<sup>3</sup>, and Yoonchang Han<sup>1</sup>

<sup>1</sup>Cochlear.ai, <sup>2</sup>Seoul National University, <sup>3</sup>SK Telecom

## ABSTRACT

Most of existing audio fingerprinting systems have limitations to be used for high-specific audio retrieval at scale. In this work, we generate a low-dimensional representation from a short unit segment of audio, and couple this fingerprint with a fast maximum inner-product search. To this end, we present a contrastive learning framework that derives from the segment-level search objective. Each update in training uses a batch consisting of a set of pseudo labels, randomly selected original samples, and their augmented replicas. These replicas can simulate the degrading effects on original audio signals by applying small time offsets and various types of distortions, such as background noise and room/microphone impulse responses. In the segment-level search task, where the conventional audio fingerprinting systems used to fail, our system using 10x smaller storage has shown promising results. Our code and dataset will be available.

**Index Terms**— acoustic fingerprint, audio search, self-supervised learning, data augmentation

## 1. INTRODUCTION

Audio fingerprinting is a content summarization technique that links short snippets of unlabeled audio contents to the same contents in the database [1]. The most well-known application is the music fingerprinting system [1–8] that enables users to identify unknown songs from the microphone or streaming audio input. Other applications include detecting copyrights [3], deleting duplicated contents [9], monitoring broadcasts [1, 10], and tracking advertisements [11].

General requirements for audio fingerprinting system are *discriminability* over a huge number of other fingerprints, *robustness* against various types of acoustic distortions, and *computational efficiency* for processing large-scale database. To achieve these requirements, most of conventional approaches [1–7] employed a novelty function to extract sparse representations of spectro-temporal features from a pre-defined audio window. These sparse representations, or acoustic landmarks [5], used to be coupled with binary hashing algorithms [1, 2, 12] for scalable search in *hamming* space.

Still, the representation learning approach to audio fingerprinting has not been discovered well. *Now-playing* [8] has been pioneering work in the direction. They trained a neural network using semi-hard triplet loss, which derived from face recognition [13]. In their setup [8], *Now-playing* could identify songs within 44h long audio database. In our benchmark, we replicate this semi-hard triplet approach and compare it with our work in a new setup: high-specific audio retrieval in a 180 times larger database.

We present a neural audio fingerprinter for robust high-specific audio retrieval based on contrastive learning. Our fingerprinting model in Figure 1 differs from the prior works in three key aspects:

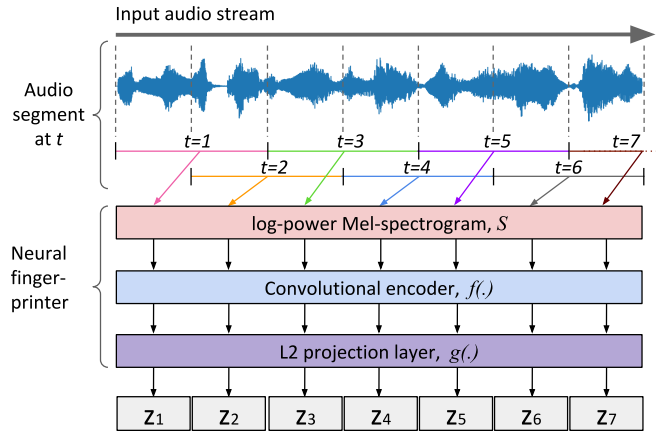


**Fig. 1.** Overview of the neural audio fingerprinter. We generate segment-wise embeddings  $z_t \in \mathcal{Z}$  that can represent a unit segment of audio from the acoustic features  $S$  at time step  $t$ . In our framework, each segment can be searched by maximum inner-product.

- Prior works [1–8] have focused on song-level audio retrieval from a music excerpt; we challenge a high-specific audio search by allowing miss-match less than 250 ms from a few seconds input.
- We introduce the contrastive learning framework for simulating maximum inner-product search (MIPS) in mini-batch.
- We employ various types of data augmentation methods for generating acoustic distractors and show their benefits to training a robust neural audio fingerprinter.

## 2. NEURAL AUDIO FINGERPRINTER

Our neural audio fingerprinter in Figure 1 transforms and maps the segment-level acoustic features into  $L^2$ -normalized space, where the inner-product can measure similarities between segments. It consists of a pre-processor and neural networks.

As a first step, input audio  $\mathcal{X}$  is converted to time-frequency representation  $\mathcal{S}$ . It is then fed into convolutional encoder  $f(\cdot)$  which is based on the previous study [8]. Finally,  $L^2$ -normalization is applied to its output through a linear projection layer  $g(\cdot)$ . Thus, we employ  $g \circ f : \mathcal{S} \mapsto \mathcal{Z}^d$  as a segment-wise encoder that transforms  $\mathcal{S}$  into  $d$ -dimensional fingerprint embedding space  $\mathcal{Z}^d$ . The  $d$ -dimensional output space  $\mathcal{Z}^d$  always belongs to *Hilbert* space  $L^2(\mathbb{R}^d)$ : the cosine similarity of a pair unit such as  $\cos(z_a, z_b)$  becomes inner-product  $z_a^T z_b$ , and due to its simplicity,  $L^2$  projection

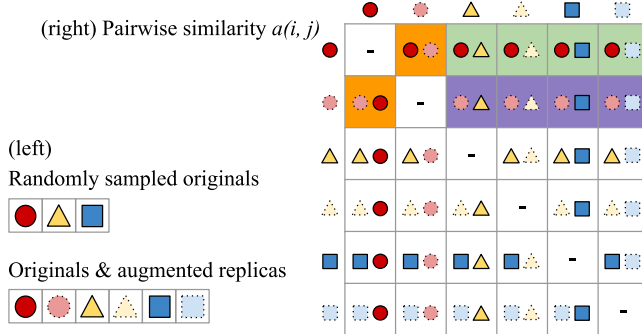


**Fig. 2.** Illustration of the contrastive prediction task in Section 2.1. (left) Batch size  $N = 6$ . We prepare  $N/2$  pairs of original/replica. The same shapes with solid/dashed lines represent the positive pair of original/replica, respectively. (right) Each element in the matrix represents pairwise similarity. In each row, a prediction task can be defined as classifying a positive pair (one of the orange squares) against the negative pairs (green or purple squares) in the same row.

has been widely adopted in metric learning studies [8, 13, 14].

The  $g \circ f(\cdot)$  described here can be interpreted as a reorganization of the previous audio fingerprinting networks [8] into the common form employed in self-supervised learning (SSL) [14–17]. However, our approach differs from the typical SSL that throws  $g(\cdot)$  away before fine-tuning for the target task: we maintain the self-supervised  $g(\cdot)$  up to the final target task.

## 2.1. Contrastive learning framework

From the previous section, we can use the inner-product as a measure of similarity between  $z_t \in \mathcal{Z}^d$  for any time step  $t$ . Without losing generality, searching the most similar point (\*) of database  $V = \{v_i\}$  for a given query  $q$  in  $\mathcal{Z}^d$  space can be formulated as maximum inner product search (MIPS),  $v_i^* := \arg \max_i (q^\top v_i)$ .

We simulate MIPS in a mini-batch setup that takes into account various acoustic distortions and input frame mismatches occurring in the fingerprint task. Mini-batch with the size of  $N$  consist of  $N/2$  pairs of  $\{s^{\text{org}}, s^{\text{rep}}\}$ .  $s^{\text{org}}$  is the time-frequency representation of sampled audio and  $s^{\text{rep}}$  is the augmented replica of  $s^{\text{org}}$ , where  $s^{\text{rep}} = \mathcal{M}_\alpha(s^{\text{org}})$ .  $\mathcal{M}_\alpha$  is an ordered augmentation chain that consists of multiple augmentors with the random parameter set  $\alpha$  for each replica. In this configuration, the indices of original examples are always odd, and that of replicas are even. Therefore, the the batch-wise output of  $f \circ g(s)$  can be  $\{z_{2k-1}^{\text{org}}, z_{2k}^{\text{rep}}\}_{k=1}^{N/2}$ .

We give each  $k$ -th example a chance to be an anchor (or a query in MIPS) to be compared with all other examples excluding itself in the batch. We calculate the pairwise inner-product matrix between all elements in the batch  $\{z_i\}_{i=1}^N$  as  $a(i,j) = z_i^\top z_j$  for  $\forall i, j \in \{1, 2, \dots, N\}$  as Figure 2. Then, we define the contrastive prediction task for a positive pair of examples  $(i, j)$  as:

$$\ell(i, j) = -\log \frac{\exp(a_{i,j}/\tau)}{\sum_{k=1}^N \mathbb{1}(k \neq i) \exp(a_{i,j}/\tau)}. \quad (1)$$

$\mathbb{1}(\cdot) \in \{0, 1\}$  is an indicator function that returns 1 iff  $(\cdot)$  is true, and  $\tau > 0$  denotes the temperature [18] parameter for softmax. We employ Equation 1 to replace MIPS from the property: computing the top- $k$  ( $k=1$  in our setup) predictions in the softmax function is

---

### Algorithm 1: Training of neural audio fingerpointer

---

```

Config: even number of batch size  $N$ , temperature  $\tau$ 
Variables: input  $s$ , representation  $z \in \mathbb{R}^d$ 
Augmentor:  $\mathcal{M}_\alpha(\cdot)$  with parameters  $\alpha$ 
Nets: encoder  $f(\cdot)$ ,  $L^2$  projection layer  $g(\cdot)$ 
1 for each sampled mini-batch  $\{s_k\}_{k=1}^{N/2}$  do
2   for  $\forall k \in \{1, \dots, N/2\}$  do
3      $z_k^{\text{org}} = g \circ f(s_k)$ 
4      $z_k^{\text{rep}} = g \circ f(\mathcal{M}(s_k))$ 
5      $z = \{z_1^{\text{org}}, z_1^{\text{rep}}, \dots, z_{N/2}^{\text{org}}, z_{N/2}^{\text{rep}}\}$ 
6     for  $\forall i \in \{1, \dots, N\}$  and  $\forall j \in \{1, \dots, N\}$  do
7        $a_{i,j} = z_i^\top z_j$  /* Pairwise similarity */
8        $\ell(i, j) = \text{NTxent}(a_{i,j}, \tau)$  /* Eq.(1) */
9     Update  $f, g$  to minimize  $\mathcal{L} \approx \frac{1}{N} \sum_{i=1}^N \ell$  /* Eq.(2) */
10   return fingerpointer  $g \circ f(\cdot)$ 

```

---

equivalent to the MIPS. A similar approach is found in [19]. The total loss  $\mathcal{L}$  averages  $\ell$  across all positive pairs, both  $(i, j)$  and  $(j, i)$ :

$$\mathcal{L} = \frac{1}{N} \sum_{k=1}^N [\ell(2k-1, 2k), \ell(2k, 2k-1)]. \quad (2)$$

Updating rules are summarized in Algorithm 1.

It is worth comparing our approach to SimCLR [14] for visual representation. Our approach differs from SimCLR on how to construct positive pairs. We use  $\{\text{original}, \text{replica}\}$ , whereas SimCLR uses  $\{\text{replica}, \text{replica}\}$  from the same original source. In our case, the anchor is already given because the database will always store the clean source, so it can be more important to learn the consistent relation between the original and its replica over all other negatives.

## 2.2. Sequence search

Our model trained by simulating MIPS is optimized for segment-level search. In the case of searching for a query sequence  $\{Q_{i=0}^L\}$  consisting of  $L$  consecutive segments: We first gather the top  $k$  segment-level search results indices  $I_{q_i}$  for each  $q_i$  from the DB. The offset is then compensated by  $I'_{q_i} = I_{q_i} - i$ . The set of candidate indices  $c \in C$  is determined by taking unique elements of  $I'_{q_i}$ . The sequence-level similarity score is the sum of all segment-level similarities from the segment index range  $[c, c + L]$ , and the index with the highest score is the output of the system.

## 3. EXPERIMENTAL SETUP

### 3.1. Dataset

The main experiment in Table 3 is reproducible with the following three data sets, which are isolated from each other.

- Train (10K-30s): A subset of the `fma_medium` [20] consisting of 30 s audio clips from a total of 10K songs.
- Test-Dummy-DB (100K-full-db): a subset of the `fma_full` [20] consisting of about 278 s audio clips from a total of 100K songs. We scale the search experiment with this.
- Test-Query/DB (500-30s): Test-DB is another subset of the `fma_medium`, which is 500 audio clips of 30 s each. Test-Query was synthesized using Test-DB as directed in Section 3.5.

**Table 1.** Fingerprinter (FP) network structure in Section 3.3.

$SC_{k*s}^{o \leftarrow i}(\cdot) := \text{ReLU} \triangleleft \text{LN} \triangleleft C_{k'*s'}^{o \leftarrow i} \triangleleft \text{ReLU} \triangleleft \text{LN} \triangleleft C_{k*s}^{o \leftarrow i}(\cdot)$
$f(\cdot) := SC_{3*2}^{h \leftarrow h} \triangleleft SC_{3*2}^{h \leftarrow 4d} \triangleleft SC_{3*2}^{4d \leftarrow 4d} \triangleleft SC_{3*2}^{4d \leftarrow 2d} \triangleleft$
$SC_{3*2}^{2d \leftarrow 2d} \triangleleft SC_{3*2}^{2d \leftarrow d} \triangleleft SC_{3*2}^{d \leftarrow d} \triangleleft SC_{3*2}^{d \leftarrow 1}(\cdot)$
$g(\cdot) := \text{L2} \triangleleft \text{Concat} \triangleleft C_{1*1}^{1 \leftarrow u} \triangleleft \text{ELU} \triangleleft C_{1*1}^{u \leftarrow v} \triangleleft \text{Split}^{h/d}(\cdot)$
$\text{FP} := g \triangleleft f(\text{input} := s_t)$

### 3.2. Data pipeline with augmentation chain

A batch consists of  $\{x^{\text{org}}, x^{\text{rep}}\}$  pairs. Each  $x^{\text{rep}}$  is generated from its corresponding  $x^{\text{org}}$  through augmentation steps as following order:

- Time offset modulation: To simulate possible discrepancies in real world search scenarios, we define positive examples as 1 s audio clips with an offset of up to  $\pm 200$  ms. We first sample 1.2 s of audio and then  $\{x^{\text{org}}, x^{\text{rep}}\}$  are chosen by random start positions.
- Background mixing: A randomly selected noise in the SNR range of [0, 10] dB is added to the audio to reflect the actual noise. The noise dataset consists of 4.3 h of a subset of AudioSet [21] and 2.3 h of pub and cafe noise recorded by us. The AudioSet was crawled within *subway*, *metro*, and *underground* tags with no music-related tags. Each dataset is split into 8:2 for train/test.
- IR filters: To simulate the effect of diverse spatial and microphone environments, microphone and room impulse response (IR) are sequentially applied by convolution operation. Public microphone [22] and spacial [23] IR dataset are split into 8:2 for train/test.
- Cutout [24] and Spec-augment [25] are applied after extracting log-power Mel-spectrogram features, such that  $\{s^{\text{org}}, s^{\text{rep}}\}$ . Unlike other augmentations, we uniformly apply a batch-wise random mask to all examples in a batch including  $s^{\text{org}}$ . The size and position of each rectangle/vertical/horizontal mask is random in the range [1/10, 1/2] the length of each time/frequency axis.

### 3.3. Network structure

In Table 1, a space-saving notation  $C_{k*s}^{o \leftarrow i}$  denotes Conv2d with input channel  $i$ , output channel  $o$ , kernel size  $1 \times k$ , and stride  $1 \times s$ . The  $k'$  and  $s'$  denotes rotation as  $k \times 1$  and  $s \times 1$ .  $\text{Split}^{h/d}$  splits input dimension  $h$  into  $d$  parts of each output dimension  $v = h/d$ .  $g \triangleleft f(\cdot)$  is  $g(f(\cdot))$ . The network parameters  $\{d, h, u, v\}$  are in Table 2.

- **Convolutional encoder  $f(\cdot)$ :**  $f(\cdot)$  takes as input a log-power Mel-spectrogram  $s_t$  with a time step  $t$  representing 1s audio captured by 50% overlapping window.  $f(\cdot)$  consists of several blocks containing spatially separable convolution (SC) [26] followed by a layer normalization (LN) [27] and a ReLU activation.
- **$L^2$  projection layer  $g(\cdot)$ :** We take the split-head from the input embeddings and pass it through the separate Linear-ELU-Linear layers for each split as in previous studies [8, 28]. After concatenating the multi-head outputs, we apply  $L^2$ -normalization.

### 3.4. Implementation details

The replication of *Now-playing* and our work shared the short-time Fourier transform (STFT) settings listed in Table 2. Note that, due to ambiguity in the previous study [8], the STFT parameters were set by us. We trained *Now-playing* with online semi-hard triplet loss [13] with the batch size  $N = 320$ .

**Table 2.** Shared configurations for experiments

Parameter	Value
Sampling rate	8,000 Hz
STFT window function	<i>Hann</i>
STFT window length and hop	1024, 256
STFT spectrogram size $Ft \times T$	$512 \times T (T = 32)$
log-power Mel-spectrogram size $Ft \times T$	$256 \times T (T = 32)$
Dynamic range	80 dB
Frequency {min, max}	{300, 4,000} Hz
Fingerprint {window length, hop}	{1s, 0.5s} or {2s, 1s}
Fingerprint dimension $d$	64 or 128
Network parameters $\{h, u, v\}$	{1024, 32, $h/d$ }
Batch size $N$	120 or 320 or 640

We trained our model using LAMB [29] optimizer, which achieved 2 pp better results with the 3 s query sequence for batch size  $N \geq 320$ . In practice, Adam [30] worked better only for  $N \leq 240$ . The learning rate had an initial value of  $1e-4 \cdot N/640$  with cosine decay without warmup [31] or restarts [32], then it reached a minimum value of  $1e-7$  in 100 epochs. The temperature in Eq.1 was  $\tau = 0.05$ , and we did not observe a meaningful performance change in the range [0.01, 0.1]. The training finished in about 30 h with a single *NVIDIA RTX 6000* GPU or Cloud TPUv3-8.

The search algorithm in Section 2.2 was implemented using an open library [33]. We used the inverted file (IVF) index structure with product quantizer (PQ) as a non-exhaustive MIPS. The IVF-PQ had 200 centroids with the code size of  $2^6$ , and 8-bits per index. In this setting, the loss of recall remained below 0.1% compared to the exhaustive search of 100K songs ( $\approx 56$ M segments) database.

### 3.5. Evaluation protocol

- Evaluation metric: To measure the performance in segment/song-level search in Section 4, we use *Top-1 hit rate(%)*:

$$100 \times \frac{(n \text{ of hits @Top-1})}{(n \text{ of hits @Top-1}) + (n \text{ of miss @Top-1})}, \quad (3)$$

which is equivalent to *recall*. In Table 3, *exact match* is the case when the system finds the correct index in database. We further define the tolerance range for *near match* as  $\pm 500$  ms.

- Test-Query generation: 2K query-sources for each {1, 2, 3, 5, 6, 10} s length are randomly cropped from Test-DB containing 500 clips of 30s each. Each query is synthesized through the random augmentation pipeline as described in Section 3.2. Note that we exclude Cutout and Spec-augment. The default SNR range is [0, 10] dB. We make sure that the data used for background mixing and IR as unseen to our model by isolating them from training set.

## 4. RESULTS AND DISCUSSION

### 4.1. Experimental results

The main results are listed in Table 3. Our implementation of the *Now-playing* [8] based on semi-hard triplet [13] took 2 s as a unit audio segment. The modified *Now-playing* with 1 s unit audio segment could be more fairly compared with our works.

**VS. *Now-playing* (semi-hard triplet)** Modified *Now-playing* consistently performed better than the replicated *Now-playing*. While cutting the dimension in half, this trend was maintained. Considering that the DB size was the same when the number of fingerprint dimensions was half, it could be seen that constructing DB with 1

**Table 3.** Top-1 hit rate (%) of large-scale (total of 100K songs) segment-level search.  $d$  denotes the dimension of fingerprint embedding. *exact match* means that our system finds the exact index. *near match* means a mismatch within  $\pm 1$  index or  $\pm 500$  ms.

Method	$d$	match	Query length in seconds					
			1 s	2 s	3 s	5 s	6 s	10 s
<i>Now-playing</i> (replicated)	128	exact	-	44.3	60.1	73.6	81.0	86.1
		near	-	46.8	63.5	75.2	81.6	86.3
<i>Now-playing</i> (modified for 1 s unit)	64	exact	25.8	58.5	69.3	78.5	81.4	87.7
		near	30.9	61.3	71.2	79.5	82.2	88.3
This work ( $N=640$ )	128	exact	26.3	58.2	69.5	78.4	81.4	87.8
		near	30.9	61.1	71.8	79.8	83.0	89.2
	64	exact	54.6	78.9	85.4	90.4	92.0	94.9
		near	61.3	81.7	86.7	90.9	92.7	95.1
This work ( $N=320$ )	128	exact	<b>62.2</b>	<b>83.2</b>	<b>87.4</b>	<b>92.0</b>	<b>93.3</b>	<b>95.6</b>
		near	68.3	84.9	88.7	92.7	94.1	95.8
This work ( $N=120$ )	128	exact	61.0	82.2	87.1	91.8	93.1	95.2
		near	67.1	84.1	88.1	92.5	93.9	95.5

**Table 4.** Effect of fingerprint dimension  $d$  in 1 s segment search.

$d$	16	32	64	128
Top-1 hit rate (%) @ 1 s	11.6	40.2	54.6	62.2

s was more advantageous to segment search. The proposed model with a 128-dimensional fingerprint using batch size of 640 always showed the best performance (highlighted in Table 3) for any query length. This confirmed that the proposed contrastive learning approach outperformed over the semi-hard triplet approach.

**Embedding dimension** In Table 2, increasing the embedding dimension  $d$ : 64→128 for the modified *Now-playing* did not affect the results significantly. In contrast, increasing the embedding dimension  $d$ : 64→128 for our best model gave us a larger improvement of exact match performance as  $\uparrow 7.6$  (54.6→62.2%) pp for the 1 s query. This reaffirmed the training benefits of our contrastive learning over the semi-hard triplet, fairly compared using the same network structure. In Table 4, we further investigated the effect of reducing  $d$  to our model with 1 s query length. We could observed a rapid drop in exact match performance while decreasing  $d$ : 64→32→16.

**Performance of sequence search** The longer the query sequence, the better the performance in all experiments. In Table 3, segment-level hit rate of our best model (highlighted) was increasing as 62.2→83.4→92.0→95.6% while increasing the query length by almost double. Thus, the longer query length was useful. In Table 3, the performance difference between near and exact match result of our best model at 1 s query was 6.1 (62.2 and 68.3%) pp. This interval decreased immediately as the query length became larger than 1. These results showed that our sequence search method introduced in Section 2.2 was quite effective.

**Effect of batch size** The larger the batch size, the better the performance in all experiments. In Table 3, reducing the batch size  $N$ : 640→120 from our best model degraded the exact match performance by  $\downarrow 6.3$  (62.2→55.9%) pp at 1 s query length. Recent works [14, 16, 17] on contrastive learning has been consistently reporting similar trends. Our result implicated that the diversity of negative examples existing by large batch could play an important role in the contrastive learning framework.

**VS. Dejavu** We compared our work with the open-source project

*Dejavu* [34] based on the conventional method [1, 5] in the song-level search task of smaller (10K-30s) scale. 69.6% of Top-1 hit rate was achieved with *Dejavu*, a song-level search engine using a 6 s query. Our best model achieved 99.5% for song-level hit rate, and exact/near match was 98.9/99.1% at the 6 s query, respectively. Our model also achieved {83.6, 95.4, 97.4}% exact match at {1,2,3} s query. The capacity of fingerprints from *Dejavu* was about 400 MB, while ours (quantized with 1/4 compression rate) was less than 40 MB for  $d=64$ . These results suggested that our work had advantages in both performance and scalability over conventional work.

#### 4.2. Size of training set, search time and scalability

The models in Table 3 were trained with about 70 h dataset. This size was less than 1% of the total 8K h DB for test. We assumed that using the entire DB for training would be impractical—a huge number of new songs are produced every day. In additional experiment, we used 10% of the Test-dummy-DB for training a  $d=64$  model. It achieved {58.3, 81.1, 86.5, 92.4, 93.4, 96.0}% of Top-1 hit rate for the query sequence of {1, 2, 3, 5, 6, 10} s. This improved  $\uparrow 3.7$  (54.6→58.3%) pp at the 1 s query over the best model with  $d=64$  in Table 3, still lower than the result of  $d=128$ . Thus, both  $d$  and the amount of training data were the factors affecting performance.

In our best model with  $d=128$ , the final DB size was about 7.5 GB for 56M segments from total of 100K songs. We report about 1.5 s search time for parallel search of 19 segments (=10 s query) with *i9-10980XE* CPU. Expanding beyond 1 M songs would be difficult to handle with in-memory search: we could observe on-disk-search using the latest SSD was only twice as slow as in-memory-search. We reserve the industry-level scalability issues for future work.

#### 4.3. Transfer to down-stream task

We further investigated the generality of the learned embeddings by performing a downstream task, as in the typical SSL [14–17] settings. By fixing  $f(\cdot)$  and fine-tuning a linear classifier, we tried audio genre classification in *GTZAN* dataset with stratified 10-fold cross-validation. Fine-tuning on the pre-trained embeddings for fingerprint achieved 59.2% accuracy, while training from scratch achieved only 32.0%. This showed that the features encoded by  $f(\cdot)$  were linearly interpretable, which was consistent with other SSL reports [14–17]. However, our result was slightly lower than the baseline of 61.0% accuracy using MFCCs+GMM [35]. This problem might be due to the limitation of the lightweight networks with the relatively short-time analysis window.

### 5. CONCLUSIONS AND FUTURE WORK

This study presented a neural audio fingerprinter for high-specific audio retrieval. Our model was trained to maximize the inner-product between positive pairs of fingerprints through a contrastive prediction task. To this end, we explicitly sampled positive pairs to have original–replica relations by applying various augmentations to clean signals. We evaluated our model in the segment-level search task with a public database of 100K songs. In the experiment, our model performed better than the model with triplet embeddings. It was also shown that our work, using 10 times less memory than an existing work, outperformed in song-level search task. So far, these results have implied that the audio fingerprinting task would inherently have self-supervised learning potentials. The future direction of this study is to test neural audio fingerprints in industry-scale database and queries from a variety of user devices.

## 6. REFERENCES

- [1] J. Haitsma and T. Kalker, “A highly robust audio fingerprinting system.,” in *Proc. of the International Society for Music Information Retrieval (ISMIR)*, 2002, vol. 2002, pp. 107–115.
- [2] A. Wang et al., “An industrial strength audio search algorithm.,” in *Proc. of the International Society for Music Information Retrieval (ISMIR)*, 2003, vol. 2003, pp. 7–13.
- [3] P. Cano, E. Batlle, T. Kalker, and J. Haitsma, “A review of audio fingerprinting,” *Journal of VLSI signal processing systems for signal, image and video technology*, vol. 41, no. 3, pp. 271–284, 2005.
- [4] S. Baluja and M. Covell, “Waveprint: Efficient wavelet-based audio fingerprinting,” *Pattern recognition*, vol. 41, no. 11, pp. 3467–3480, 2008.
- [5] C. V. Cotton and D. P. Ellis, “Audio fingerprinting to identify multiple videos of an event,” in *Proc. of the IEEE International Conference on Acoustics, Speech and Signal Processing (ICASSP)*. IEEE, 2010, pp. 2386–2389.
- [6] J. Six and M. Leman, “Panako - A Scalable Acoustic Fingerprinting System Handling Time-Scale and Pitch Modification,” in *Proc. of the International Society for Music Information Retrieval (ISMIR)*, 2014.
- [7] T.-K. Hon, L. Wang, J. D. Reiss, and A. Cavallaro, “Audio fingerprinting for multi-device self-localization,” *IEEE/ACM Transactions on Audio, Speech, and language processing*, vol. 23, no. 10, pp. 1623–1636, 2015.
- [8] B. Gfeller, R. Guo, et al., “Now playing: Continuous low-power music recognition,” in *NeurIPS 2017 Workshop on Machine Learning on the Phone and other Consumer Devices*, 2017.
- [9] C. J. Burges, D. Plastina, J. C. Platt, E. Renshaw, and H. S. Malvar, “Using audio fingerprinting for duplicate detection and thumbnail generation,” in *Proc. of the IEEE International Conference on Acoustics, Speech, and Signal Processing (ICASSP)*. IEEE, 2005, vol. 3, pp. iii–9.
- [10] E. Allamanche, “Audiod: Towards content-based identification of audio material,” in *Proc. of the 100th AES Convention, May 2001*, 2001.
- [11] Y. Jiang, C. Wu, K. Deng, and Y. Wu, “An audio fingerprinting extraction algorithm based on lifting wavelet packet and improved optimal-basis selection,” *Multimedia Tools and Applications*, vol. 78, no. 21, pp. 30011–30025, 2019.
- [12] A. Gionis, P. Indyk, and R. Motwani, “Similarity search in high dimensions via hashing,” in *Proc. of the International Conference on Very Large Data Bases (VLDB)*, San Francisco, CA, USA, 1999, VLDB ’99, p. 518–529.
- [13] F. Schroff, D. Kalenichenko, and J. Philbin, “Facenet: A unified embedding for face recognition and clustering,” in *Proc. of the IEEE conference on computer vision and pattern recognition (CVPR)*, 2015, pp. 815–823.
- [14] T. Chen, S. Kornblith, M. Norouzi, and G. Hinton, “A simple framework for contrastive learning of visual representations,” *arXiv preprint arXiv:2002.05709*, 2020.
- [15] A. v. d. Oord, Y. Li, and O. Vinyals, “Representation learning with contrastive predictive coding,” *arXiv preprint arXiv:1807.03748*, 2018.
- [16] T. Chen, S. Kornblith, K. Swersky, M. Norouzi, and G. Hinton, “Big self-supervised models are strong semi-supervised learners,” *arXiv preprint arXiv:2006.10029*, 2020.
- [17] A. Baevski, H. Zhou, A. Mohamed, and M. Auli, “wav2vec 2.0: A framework for self-supervised learning of speech representations,” *arXiv preprint arXiv:2006.11477*, 2020.
- [18] G. Hinton, O. Vinyals, and J. Dean, “Distilling the knowledge in a neural network,” *arXiv preprint arXiv:1503.02531*, 2015.
- [19] P. H. Chen, S. Si, S. Kumar, Y. Li, and C.-J. Hsieh, “Learning to screen for fast softmax inference on large vocabulary neural networks,” *arXiv preprint arXiv:1810.12406*, 2018.
- [20] M. Defferrard, K. Benzi, P. Vandergheynst, and X. Bresson, “Fma: A dataset for music analysis,” in *Proc. of the International Society for Music Information Retrieval (ISMIR)*, 2017.
- [21] J. F. Gemmeke, D. P. Ellis, and et al., “Audio set: An ontology and human-labeled dataset for audio events,” in *Proc. of the IEEE International Conference on Acoustics, Speech and Signal Processing (ICASSP)*. IEEE, 2017, pp. 776–780.
- [22] Xaudia, “Microphone impulse response project,” 2017, [Online]. <http://micirp.blogspot.com/>.
- [23] M. Jeub, M. Schafer, and P. Vary, “A binaural room impulse response database for the evaluation of dereverberation algorithms,” in *Proc. of the International Conference on Digital Signal Processing (ICDSP)*. IEEE, 2009, pp. 1–5.
- [24] T. DeVries and G. W. Taylor, “Improved regularization of convolutional neural networks with cutout,” *arXiv preprint arXiv:1708.04552*, 2017.
- [25] D. S. Park, W. Chan, et al., “Specaugment: A simple data augmentation method for automatic speech recognition,” in *Proc. of the Interspeech*, 2019, pp. 2613–2617.
- [26] F. Mamalet and C. Garcia, “Simplifying convnets for fast learning,” in *Proc. of the International Conference on Artificial Neural Networks (ICANN)*. Springer, 2012, pp. 58–65.
- [27] J. L. Ba, J. R. Kiros, and G. E. Hinton, “Layer normalization,” *arXiv preprint arXiv:1607.06450*, 2016.
- [28] H. Lai, Y. Pan, Y. Liu, and S. Yan, “Simultaneous feature learning and hash coding with deep neural networks,” in *Proc. of the IEEE conference on computer vision and pattern recognition (CVPR)*, 2015, pp. 3270–3278.
- [29] Y. You, J. Li, S. Reddi, et al., “Large batch optimization for deep learning: Training bert in 76 minutes,” in *Proc. of the International Conference on Learning Representations (ICLR)*, 2019.
- [30] D. P. Kingma and J. Ba, “Adam: A method for stochastic optimization,” *arXiv preprint arXiv:1412.6980*, 2014.
- [31] P. Goyal, P. Dollár, R. Girshick, P. Noordhuis, L. Wesolowski, A. Kyrola, A. Tulloch, Y. Jia, and K. He, “Accurate, large minibatch sgd: Training imagenet in 1 hour,” *arXiv preprint arXiv:1706.02677*, 2017.
- [32] I. Loshchilov and F. Hutter, “Sgdr: Stochastic gradient descent with warm restarts,” *arXiv preprint arXiv:1608.03983*, 2016.
- [33] J. Johnson, M. Douze, and H. Jégou, “Billion-scale similarity search with gpus,” *IEEE Transactions on Big Data*, 2019.
- [34] W. Drevo, “Dejavu: open-source audio fingerprinting project,” 2014, [Online]. <https://pypi.org/project/PyDejavu/>.
- [35] G. Tzanetakis and P. Cook, “Musical genre classification of audio signals,” *IEEE Transactions on speech and audio processing*, vol. 10, no. 5, pp. 293–302, 2002.